Sulfur deactivation and regeneration of mono- and bimetallic Pd-Pt methane oxidation catalysts

Monique Shauntá Wilburn, William S. Epling [*],[1]

Department of Chemical and Biomolecular Engineering, University of Houston, United States

ABSTRACT

Complete CH_4 oxidation (combustion) studies were conducted with Pt/Pd mono- and bimetallic, γ-Al_2O_3 supported catalysts before and after exposure to SO_2. CO and SO_2 adsorption DRIFTS studies were used to identify sites that adsorbed SO_2 and evaluate the Pd:Pt mole ratio effect on sulfur surface species formation. Temperature-programmed oxidation, desorption, and reduction as models for possible catalyst regeneration were evaluated in terms of sulfur release and CH_4 oxidation performance recovery. At low temperatures, Pd-rich catalysts, i.e. with little to no Pt substitution, tended to form aluminum sulfate species, which could be removed at high temperatures to recover catalytic activity. In contrast, catalysts with higher Pt content were less effective at sulfate formation at low temperatures. In this case, molecular SO_2 and aluminum surface sulfite species inhibited the CH_4 oxidation reaction over a broader temperature range. In general, for the bimetallic samples the effectiveness of SO_2 regeneration methods decreased with increasing Pt content. Also, for bimetallic catalysts with higher Pt content, the associated sintering effects from the temperature programmed regeneration methods were more significant.

© 2017 Elsevier B.V. All rights reserved.

1. Introduction

Natural gas contains methane, other hydrocarbons, such as ethane and propane [1–3], and trace level species including sulfur species [4]. In comparison with diesel engines, natural gas engine combustion produces lower CO_2, CO, NO_x, and soot emissions. One concern is of course the associated methane emissions and methane's greenhouse gas potential. A typical approach to mitigate such emissions would be the installation of an exhaust stream oxidation catalyst. Over such, under lean-burn conditions heavier hydrocarbons can be completely oxidized at low temperatures [3] but high temperatures are necessary for complete methane conversion [4]. However, lean-burn natural gas engine exhaust temperatures are relatively low (i.e. 300–500 °C) [1,5], resulting in methane slip. Furthermore, those trace sulfur species deactivate methane oxidation catalysts resulting in reduced catalytic activity with time-on-stream and thus increased levels of unconverted methane in natural gas engine exhaust [6].

There has been a substantial amount of CH_4 oxidation research published, with a comprehensive review of these by Gélin and Primet [4]. Specific challenges discussed in their review article include thermal sintering due to the required CH_4 oxidation temperature, the low CH_4 concentrations in the exhaust, H_2O inhibition, and degradation via sulfur poisoning. Studies have shown that for O_2:CH_4 molar ratios exceeding 2, i.e. lean-burn operation conditions, PdO-based catalysts are significantly more active than Pt-based catalysts [4]. Interestingly, under rich conditions, i.e. when there are stoichiometric or sub-stoichiometric amounts of O_2 relative to CH_4, Pt has been found to be more active [7]. The literature shows that substituting Pt for Pd, i.e bimetallics, results in catalysts with improved resilience with time on stream [8–15], and even small substitutions (7–10% Pt for Pd) provides some sintering resistance and increased catalytic activity [11,14,] in comparison to monometallic Pd catalysts. Thus there are known benefits of bimetallic systems for CH_4 oxidation.

In terms of sulfur poisoning/deactivation, it is well known that Pd-based catalysts are quite susceptible to sulfur. In one example, CH_4 oxidation on fresh and hydrothermally aged Pd/Al_2O_3 catalysts was evaluated. When 1 ppm SO_2 was added to the feed, the activity declined similarly for both catalysts [16]. In contrast to the abrupt decay in Pd-based catalyst activity upon SO_2 exposure [16], Lapisardi et al. found that CH_4 oxidation activity gradually declined for Pt/Al_2O_3 catalysts when exposed to H_2S [6].

Ottinger and coworkers studied sulfur regeneration of a Pd-based CH_4 oxidation catalyst via high temperature exposure as well as via a reductive treatment. They found that for the thermal regen-

eration, temperatures greater than 500 °C were required to regain some activity, whereas the reductive treatment provided better regeneration efficiency [17]. Similarly, Arosio et al. [18] showed that, for Pd-based catalysts, higher temperatures (>750 °C) were required for sulfur regeneration in the presence of simulated lean-CH_4 oxidation conditions, but switching from this lean atmosphere to one which was CH_4 rich resulted in much lower temperatures required to recover activity.

Although bimetallic Pt/Pd catalysts show resistance to sintering and improved activity, researchers found that the bimetallic activity benefit only held true in the absence of sulfur [6]. Interestingly, SO_2 poisoning of a Pt/Pd bimetallic sample resulted in decreased activity, but a pre-reduction prior to SO_2 exposure had significantly less impact [15]. Since aluminum surface and bulk sulfates are stable up to 650 °C [19] and 800–920 °C [20] respectively, it is likely that sulfur species will compromise activity to some extent until these species can be decomposed at high temperatures. Although some researchers reported that aluminum sulfates are quite resistant to reduction [20], others found that aluminum sulfates, which thermally decompose above 800 °C, can be reduced in H_2 at 600 °C [19].

In this study three approaches based on gas environment were evaluated for CH_4 oxidation activity regeneration, which should correlate to sulfur species decomposition. Here we focused on evaluating model sulfur regeneration methods as a function of Pd:Pt mole ratio.

2. Experimental methods

2.1. Catalyst preparation and reactor experimental set-up

The precursors, $Pd(NO_3)$ and $Pt(NH_3)_4(NO_3)_2$, and Puralox γ-Al_2O_3, were procured from Sigma-Aldrich. Using the incipient wetness impregnation method, the following Pd-Pt/Al_2O_3 powder catalysts were prepared: $Pd_{1.0}Pt_{0.0}/Al_2O_3$, $Pd_{0.9}Pt_{0.1}/Al_2O_3$, $Pd_{0.7}Pt_{0.3}/Al_2O_3$, $Pd_{0.3}Pt_{0.7}/Al_2O_3$, and $Pd_{0.0}Pt_{1.0}/Al_2O_3$. All catalysts contained the same total number of precious metal (PM) moles used to synthesize a 1 wt.% Pd/Al_2O_3 catalyst. After drying overnight, all samples were calcined in air at 550 °C.

For all reactor pretreatment and experimental conditions, 29.3 mg of active catalyst was used with a 200 mL/min flow, to achieve an equivalent monolith space velocity of 50,000 h^{-1} assuming a 2 g/in^3 loading. The active catalyst mass was diluted with silica beads to prevent dense packing and hot spots within the catalyst bed. Each sample was installed in a 4 mm diameter quartz tube. Quartz wool was placed at both catalyst bed ends to secure the bed particles, maintain the catalyst bed position in the quartz tube, and maintain the 20 mm catalyst bed length. Prior to experiments, all samples underwent an oxidation pretreatment at 100 °C with 10 vol.% O_2 in N_2 for 5 min, and were then heated to 400 °C and reduced under 5 vol.% H_2 in N_2 for 30 min. Following reduction, the reactor was purged with N_2 only for 30 min prior to being cooled to 35 °C. Using a Valco pulse injection valve, 10 μL doses of CO were injected into the reactor at regular intervals. When the CO injection pulse-signature ceased to change with each additional CO pulse injection, as measured by an MKS FTIR 2030, the sample was considered saturated. After saturation was achieved, the total CO uptake volume was used to determine the sample PM dispersion and corresponding particle size. The dispersion values for fresh monometallic samples were comparable to those obtained during validation with a Micromeritics ASAP 2020 Chemisorption system. Preliminary data demonstrate that sulfur interactions are influenced by particle size. To avoid this complexity in the data analysis, all samples for this study contained particles in the same particle size range.

Each catalyst sample was then pretreated with 2000 ppm CH_4 and 10 vol.% O_2 in N_2 until CH_4 conversion stabilized, assumed to be when the CH_4 conversion ceased to change while the gas temperature and feed gas concentration were kept constant. All catalyst samples containing any Pd were stabilized at ~500 °C. The monometallic Pt sample was stabilized at ~650 °C because methane combustion did not occur until higher temperatures were reached in this case. Catalysts having been prepared through this protocol are referred to as fresh catalyst samples.

Bronkhorst and MKS mass flow controllers were used to control the inlet gas flowrates. For all reactor experiments, the gas concentrations at the catalyst bed outlet were measured using an MKS MultiGas 2030 FTIR Spectrometer gas analyzer. A Thermoscientific Lindberg/Blue tube furnace was used to set and control the temperature of the catalyst bed. Type K thermocouples were placed at the catalyst bed inlet and outlet to measure the inlet and outlet gas temperatures.

All catalytic activity assessments used the same reference temperature-programmed oxidation (TPO) protocol: 2000 ppm CH_4 and 10 vol.% O_2 in N_2 with a 5 °C/min temperature ramp rate. Following the pretreatment under reactants, each sample underwent a reference TPO to obtain a baseline of its fresh catalytic activity. After each regeneration procedure, the reference TPO was performed again in an effort to compare the initial catalytic activity to that observed following regeneration.

Each sample was exposed to 30 ppm SO_2 and 10 vol.% O_2 in N_2 at 100 °C. After SO_2 saturation was achieved, the reactor was purged with N_2 at 100 °C to reduce the residual SO_2 in the reactor system lines and remove weakly adsorbed SO_2 from the sample.

2.2. Sulfur regeneration

After the SO_2 exposure, each catalyst sample underwent one of the following regeneration methods.

1. Selected samples underwent the reference TPO protocol. CH_4 oxidation and SO_2 desorption were monitored during the temperature ramp. The SO_2 release characteristics helped define experimental conditions for SO_2 DRIFTS studies, to be discussed below.
2. Temperature-programmed desorption (TPD) was performed to determine at what temperatures under inert conditions sulfur species would decompose or desorb. The TPD was performed in a flow stream of N_2 only using the following protocol: a ramp rate of 10 °C/min to 900 °C followed by a hold at 900 °C for an additional 15 min.
3. Temperature-programmed reduction (TPR) was performed with selected samples up to 600 °C in a 5 vol.% H_2 in N_2 flow stream, and held there for 30 min in an attempt to reduce and decompose sulfate species. Following reduction, the reactor was purged with N_2 prior to the reoxidizing the sample in 10 vol.% O_2 in N_2 at 600 °C for 30 min.

2.3. Thermal degradation effects

After the catalyst CH_4 conversion stabilized, the sample temperature was increased in pure N_2 at a ramp rate of 10 °C/minute to 650 °C followed by a hold at 650 °C for an additional 15 min. After cooling the sample, a reference TPO was performed to assess changes in performance due to the 650 °C exposure. The above protocol was repeated for a 900 °C exposure.

Precious metal particle sizes were measured after these high temperature exposures. After the TPO reference protocol, the samples were reduced at 400 °C under a 5 vol.% H_2 in N_2 flow. Following reduction, the reactor was cooled to 35 °C. Using a Valco pulse injection valve, 10 μL of CO were injected in regular intervals. When

Table 1
Sample preparation information and particle sizes determined via pulse-injection, CO chemisorption at 35 °C.

Pd Mole [%]	Pt Mole [%]	Particle Size [nm]	Total PM Loading [wt.%]
100	0	2.0	1.0
90	10	1.6	1.1
70	30	3.2	1.2
30	70	1.4	1.6
0	100	3.9	1.8

the injection pulse-signature was consistently repeated, the sample was assumed saturated. After saturation was achieved, the total volume of CO adsorbed was used to determine the sample PM dispersion and corresponding particle size. These data were used to assess whether the high temperatures required for TPD and TPR regeneration had any negative effect on CH_4 oxidation activity.

2.4. Diffuse reflectance infrared Fourier transform spectroscopy (DRIFTS) characterization

In preparation for the DRIFTS experiments, each catalyst was aged in a 1.8 vol.% H_2O and 10 vol.% O_2 in N_2 flow stream for 8 h at 700 °C. After aging in the reactor, catalysts were transferred to a Harrick Scientific Praying Mantis DRIFTS cell. Background spectra were gathered in 50 mL/min of He only at 35 °C, 100 °C, and 300 °C. The background spectra were subtracted from their corresponding spectra obtained at each temperature during the following experiments.

Prior to experiments, each catalyst underwent an oxidation treatment at 100 °C with 10 vol.% O_2 in He for 5 min. The catalyst was then reduced at 400 °C with 5 vol.% H_2 in He for 30 min. After reduction, the catalyst was maintained at 400 °C for an additional 30 min while the cell was purged with He to minimize the residual H_2 content within the DRIFTS cell and system lines. The catalyst was then cooled to 35 °C and exposed to 1 vol.% CO and 10 vol.% N_2 in He until CO saturation. For all DRIFTS experiments, saturation was determined by a lack of change in the collected DRIFTS spectra.

The system was purged with He prior to increasing the sample temperature to 100 °C. At this temperature, all CO had desorbed based on a lack of change in the IR spectra. Each catalyst was then exposed to 100 ppm SO_2 and 10 vol.% N_2 in He at 100 °C. After the catalyst was saturated at 100 °C, the plotted SO_2 adsorption spectrum was obtained. The system was purged with He prior to decreasing the catalyst temperature to 35 °C. CO adsorption was repeated and spectra collected upon CO saturation at 35 °C. The system was then purged with He again prior to increasing the sample temperature to 300 °C. The SO_2 desorption spectrum was obtained after the DRIFTS spectra ceased to change at 300 °C. The desorption temperature, 300 °C, was selected based on sulfur release during TPD experiments discussed below. Again the system was purged with He prior to decreasing the catalyst temperature to 35 °C. CO adsorption was repeated and spectra collected upon CO saturation at 35 °C. CO adsorption spectra were collected prior to and after the SO_2 sorption DRIFTS experiments in an effort to determine the types of sites impacted by SO_2 adsorption. OMNIC software was utilized for peak deconvolution.

3. Results and discussion

3.1. Baseline catalytic activity

Prior to sulfur exposure, the samples underwent particle size measurements and a reference TPO to obtain a measure of the fresh catalytic activity. The sample preparation and characterization information as well as the kinetic regime ignition profiles
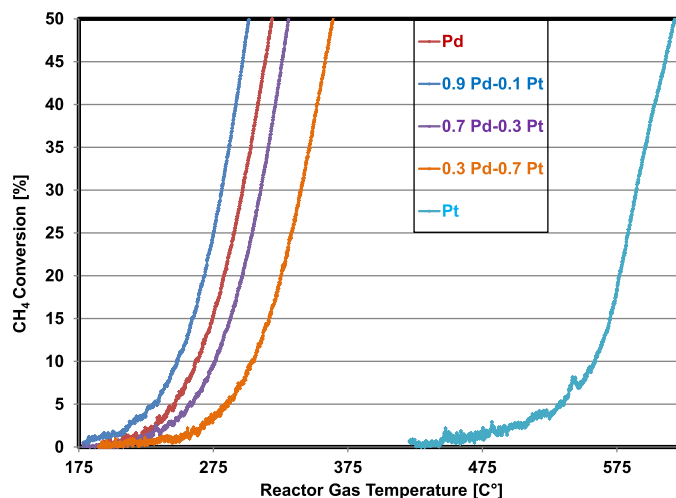
Fig. 1. CH_4 TPO over the fresh catalysts in flowing 2000 ppm CH_4 and 10 vol.% O_2 in N_2, with a ramp rate of 5 °C/min.

obtained during this experiment are compared in Table 1 and Fig. 1 respectively. Substituting some Pt into the formulation, 0.9 Pd-0.1 Pt, resulted in increased activity in comparison to monometallic Pd. Greater substitutions led to decreased activity, with the monometallic Pt sample the poorest tested. Lapisardi et al. observed similar trends for 2 wt.% Pd:Pt/Al_2O_3 catalysts [6].

3.2. Sulfur impact on catalytic activity

After SO_2 exposure, the same TPO experiment was performed to assess how SO_2 impacted catalytic activity. The ignition curves for the fresh and SO_2-exposed monometallic samples are compared in Fig. 2a. SO_2 exposure inhibited the CH_4 oxidation reaction for monometallic Pd, but monometallic Pt was unaffected by this sulfur treatment. Using T_{50} (the temperature where 50% CH_4 conversion was attained) as a metric, the changes in catalytic activities of the SO_2-exposed monometallic and bimetallic catalysts are compared in Fig. 2b. In comparison to monometallic Pd, sulfur inhibition decreased upon substituting 10% Pt into the sample, 0.9 Pd-0.1 Pt. Recalling that monometallic Pt was SO_2 resistant, it was suspected that increased substitution into Pd catalysts would result in decreased sulfur inhibition during CH_4 oxidation. Instead, similar to that observed for fresh CH_4 oxidation activity, further increases in Pt substitution led to reduced benefit, to the extent that with 70% Pt, the loss in activity with SO_2 exposure was the greatest.

In overlaying the measured sulfur desorption concentrations with the conversion plots (Fig. 3), the onset of methane oxidation was observed after a SO_2 desorption feature. Note, no SO_3 or H_2SO_4 was observed. Both the sulfur release and inhibition extents appeared to vary with Pd:Pt mole ratio.

3.3. DRIFTS studies

DRIFTS was used to characterize how the sulfur release and CH_4 oxidation inhibition varied with mole ratio. Although monometallic Pd was more active than Pt for complete CH_4 oxidation, the CH_4 oxidation reaction was inhibited at low temperatures after exposing the monometallic Pd sample to SO_2, unlike Pt. The 0.3 Pd-0.7 Pt sample was less active and less resistant to sulfur poisoning in comparison to the other characterized bimetallic samples. For these reasons, monometallic Pd and Pt as well as bimetallic 0.3 Pd-0.7 Pt samples were selected for study using DRIFTS. CO DRIFTS was used to determine how sulfur exposure impacted the PM sites. SO_2 DRIFTS was used to identify the sulfur species types formed during
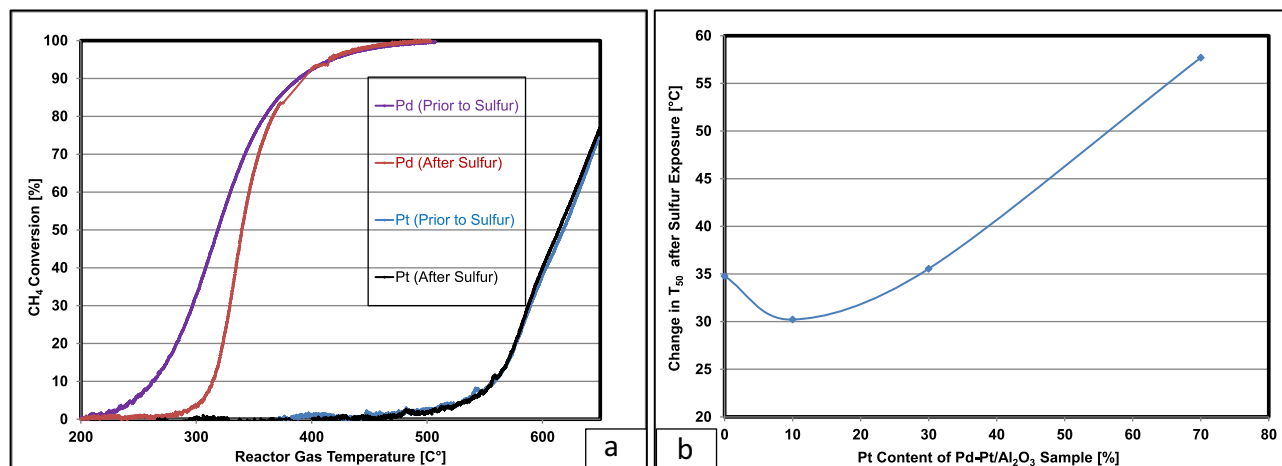
Fig. 2. CH_4 TPO in flowing 2000 ppm CH_4 and 10 vol.% O_2 in N_2, with a ramp rate of 5 °C/min. a) CH_4 conversion during the TPO for fresh and SO_2-exposed monometallic catalysts; (b) the change in CH_4 T_{50} after sulfur exposure for the monometallic Pd and bimetallic catalysts.
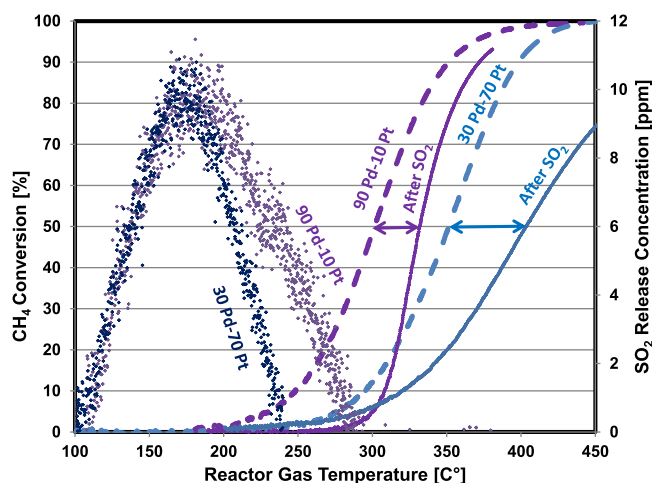
Fig. 3. SO_2 release and inhibition during TPO over the 0.9 Pd-0.1 Pt and 0.3 Pd-0.7 Pt samples in flowing 2000 ppm CH_4 and 10 vol.% O_2 in N_2, with a ramp rate of 5 °C/min.

adsorption at 100 °C and which were stable up to 300 °C, the temperature at which SO_2 release at low temperature ended, as shown in Fig. 3.

3.3.1. CO adsorption

After catalysts were saturated with CO at 35 °C, DRIFTS spectra were collected. Prior to SO_2 exposure, the Pd spectrum contained intense peaks at 2088 cm^{-1} and 1996 cm^{-1} as well as a lower intensity peak at 1936 cm^{-1} (Fig. 4a). The 2088 cm^{-1} and 1996 cm^{-1} peaks were assigned to CO linearly adsorbed on metallic Pd (Pd^0-CO) [21–24] and CO bridged across two metallic Pd atoms [22,24] respectively. The lower intensity peak corresponds to CO bridged across two partially oxidized Pd atoms (Pd$^+$-CO) [20,22,25]. After SO_2 exposure, the peaks at 1996 cm^{-1} and 1936 cm^{-1} disappeared while the peak at 2088 cm^{-1} shifted to 2102 cm^{-1} and was significantly reduced in intensity. After low-temperature desorbing sulfur species were removed via TPD to 300 °C, the sample was cooled to 35 °C and exposed to CO while spectra were collected. The peaks corresponding to CO adsorbed in a bridged manner across two metallic Pd atoms, 1998 cm^{-1}, and two partially oxidized Pd atoms, 1951 cm^{-1}, reappeared. The feature originally centered at 2102 cm^{-1} stretched, resulting in a peak position at 2127 cm^{-1}, corresponding to CO linearly adsorbed on partially oxidized Pd

(Pd^{2+}-CO). The changes in CO adsorption spectra upon sulfur exposure and after sulfur desorption up to 300 °C provide evidence that the Pd sites were covered with sulfur species during adsorption but some were re-available after the TPD to 300 °C. Though still associated with CO linearly bound adsorption sites, the peak shift to 2127 cm^{-1} shows that some reduced Pd sites were partially reoxidized, probably via the alumina support, as the sample temperature was increased to 300 °C.

Prior to SO_2 exposure, CO adsorption spectra collected from 0.3 Pd-0.7 Pt contained peaks at 2090 cm^{-1} and 1988 cm^{-1} (Fig. 5a). Not shown here for brevity, CO adsorption spectra collected from hydrothermally aged bimetallic samples with at least 30 mol% Pd (relative to Pt) displayed peaks at 2090 cm^{-1} and ~1995 cm^{-1}, which correspond to CO linear and bridged adsorption on metallic Pd sites. Due to the similarities in spectra, peaks from the 0.3 Pd-0.7 Pt sample were assigned to linear and bridged CO adsorption on metallic Pd respectively. In spite of the sample being bimetallic, no Pt features were observed, so we inferred that Pd atoms completely covered the Pt atoms [19]. After sulfur treatment, the peak at 1988 cm^{-1} disappeared while the peak at 2090 cm^{-1} shifted to 2098 cm^{-1} and was significantly reduced in intensity. Following the TPD to 300 °C, CO adsorption spectra were obtained after CO saturation. The peaks corresponding to CO adsorbed linearly, 2095 cm^{-1}, and bridged, 1981 cm^{-1}, on metallic Pd were once again detectable. A new peak evolved at 1912 cm^{-1} corresponding to CO bridged across partially oxidized Pd (Pd$_2^+$-CO) atoms [22,23]. This new peak provides evidence that some metallic Pd sites were again partially reoxidized during the temperature ramp to 300 °C. Due to the low peak intensities observed in the final 0.3 Pd-0.7 Pt CO spectra, we inferred that the Pd sites were still partially covered with sulfur species even after increasing the sample temperature to 300 °C.

Before being exposed to SO_2, the spectrum obtained after exposing the monometallic Pt sample to CO (Fig. 6a) contained a peak at 2094 cm^{-1} and a broad band from 1908 to 1830 cm^{-1}, which were assigned to CO adsorbed on Pt sites in linear [20,21] and bridged modes [22–24] respectively. Following SO_2 exposure, the CO adsorption spectrum for Pt no longer contained the broad band from 1908 to 1830 cm^{-1}. The peak at 2094 cm^{-1} also shifted to 2085 cm^{-1} and was reduced in intensity. Although there was a slight peak shift, the peak at 2085 cm^{-1} we still assign to CO linearly adsorbed on Pt sites. Following TPD to 300 °C, spectra were obtained again after CO saturation. The peaks corresponding to CO linearly adsorbed on Pt sites, 2096 cm^{-1}, reappeared, but no peaks associated with bridged CO adsorbed across Pt sites were observed. The CO spectral changes upon SO_2 exposure and after the TPD to
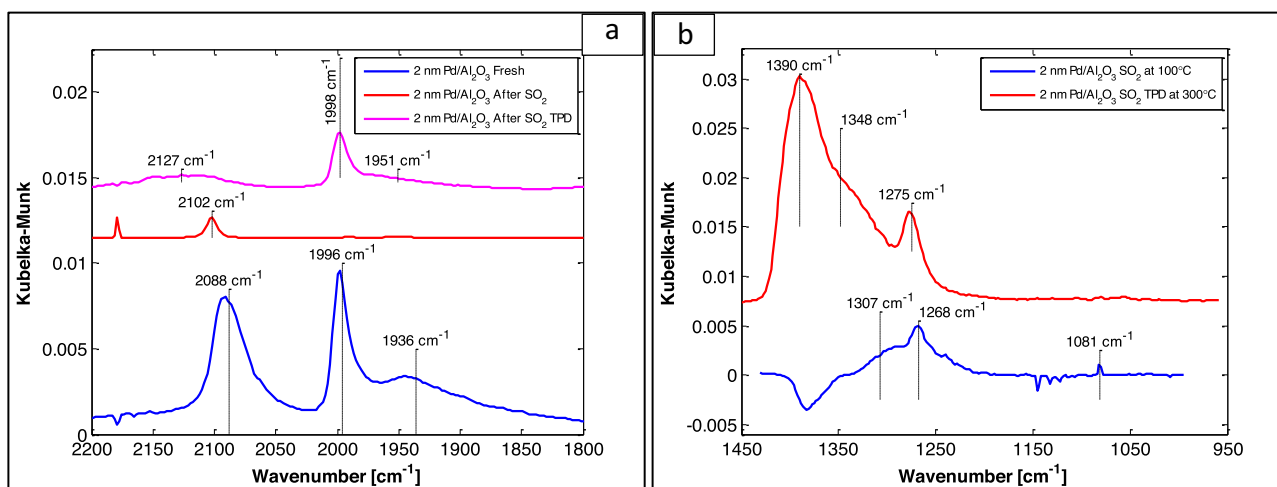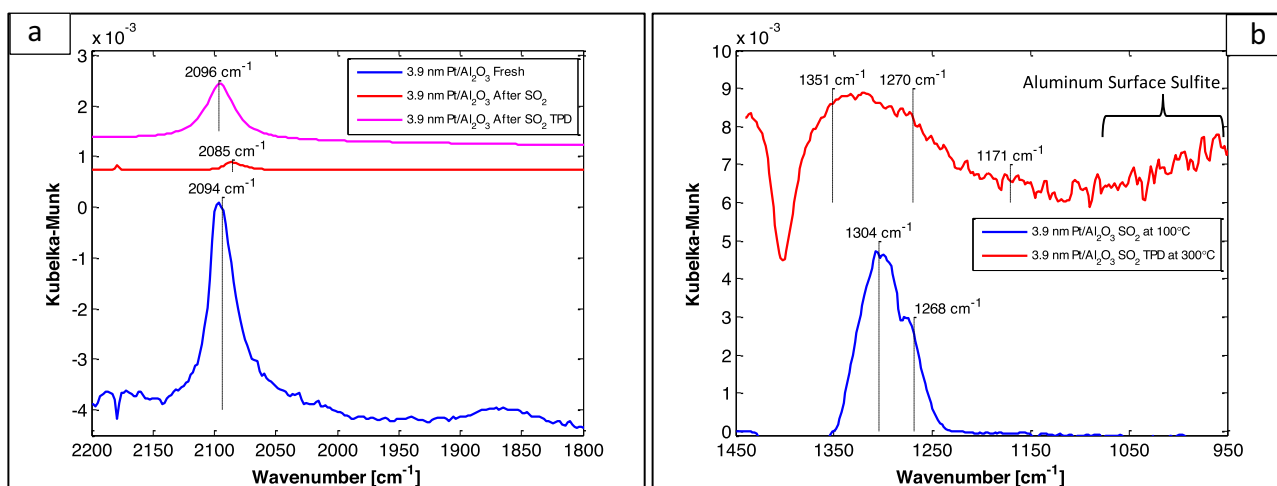
Fig. 4. DRIFTS spectra obtained from a Pd/Al$_2$O$_3$ catalyst (a) CO spectral features after CO saturation at 35 °C before and after SO$_2$ exposure, as well as after the TPD to 300 °C in N$_2$ following the SO$_2$ exposure; (b) SO$_2$ spectral features after SO$_2$ saturation at 100 °C and a subsequent TPD, in flowing N$_2$, at 300 °C.
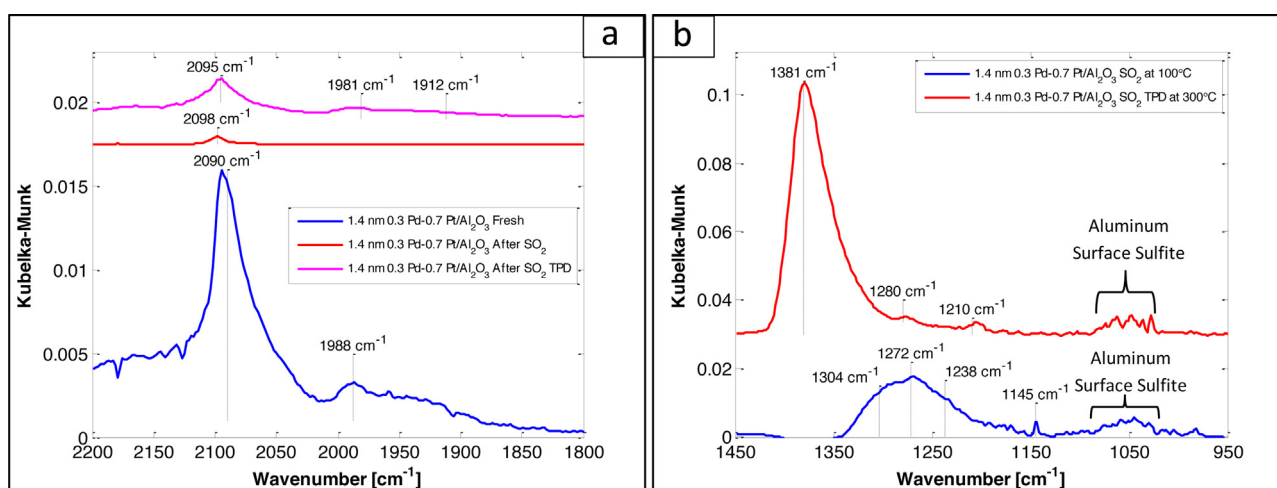
Fig. 5. DRIFTS spectra obtained from a 0.3 Pd-0.7 Pt/Al$_2$O$_3$ catalyst (a) CO spectral features after CO saturation at 35 °C before and after SO$_2$ exposure, as well as after the TPD to 300 °C in N$_2$ following the SO$_2$ exposure; (b) SO$_2$ spectral features after SO$_2$ saturation at 100 °C and a subsequent TPD, in flowing N$_2$, at 300 °C.

Fig. 6. DRIFTS spectra obtained from a Pt/Al$_2$O$_3$ catalyst (a) CO spectral features after CO saturation at 35 °C before and after SO$_2$ exposure, as well as after the TPD to 300 °C in N$_2$ following the SO$_2$ exposure; (b) SO$_2$ spectral features after SO$_2$ saturation at 100 °C and a subsequent TPD, in flowing N$_2$, at 300 °C.

Table 2
Change in T_{50} values due to TPO regeneration in flowing 2000 ppm CH_4 and 10 vol.% O_2 in N_2.

Pd Mole%	Pt Mole%	ΔT_{50} Between Fresh and TPO Regenerated Catalysts	ΔT_{50} Between SO_2 Treated and TPO Regenerated Catalysts
100	0	18.3	−16.4
90	10	14.5	−15.7
30	70	48.0	−9.7

Table 3
Change in T_{50} values after TPD regeneration in flowing N_2 up to 900 °C.

Pd Mole%	Pt Mole%	ΔT_{50} Between Fresh and TPD Regenerated Catalysts	ΔT_{50} Between SO_2 Treated and TPD Regenerated Catalysts
90	10	11.1	−22.4
70	30	34.2	−7.8
30	70	112.1	54.4

Table 4
Change in T_{50} and particle sizes after exposure to 650 °C and 900 °C in flowing N_2.

Pd Mole%	Pt Mole%	ΔT_{50} After 650 °C Exposure	ΔT_{50} After 900 °C Exposure	Factor Increase in PM Particle Size After 900 °C Exposure
90	10	−7.0	0.8	2.2
70	30	22.4	29.3	1.9
30	70	105.6	153.2	4.4

300 °C provides evidence that the metallic Pt sites that typically adsorb CO in a linear manner, were covered with SO_2 until removed at 300 °C. The Pt sites that typically adsorb CO in a bridged manner, were not detected in the CO adsorption spectra even after 300 °C exposure. We inferred that these sites still contained sulfur species which only decompose at temperatures greater than 300 °C.

3.3.2. SO_2 adsorption and desorption

During the CH_4 TPO with samples that had been exposed to SO_2, the results in Fig. 3 showed that there were differences on a mole ratio basis in the amount of sulfur species released and the temperature span over which desorption occurred. To investigate these differences, representative DRIFTS spectra were collected from Pd, 0.3 Pd-0.7 Pt, and Pt catalysts (Figs. 4b, 5b, and 6b) after SO_2 exposure at 100 °C and TPD up to 300 °C. When catalysts supported on alumina are exposed to SO_2 below 200 °C, aluminum surface sulfite species [$Al_2(SO_3)_3$] form, then molecular SO_2 chemisorbs and physisorbs on the aluminum surface and hydroxyl groups respectively [26]. During 100 °C SO_2 exposure, the spectrum obtained from the Pd sample (Fig. 4b) displayed peaks at 1307 cm^{-1}, 1266 cm^{-1}, and 1081 cm^{-1}. The peaks at 1307 cm^{-1} and 1266 cm^{-1} were assigned to physisorbed [26,27] and chemisorbed molecular SO_2 [26] respectively. The low intensity peak at 1081 cm^{-1} corresponds to aluminum surface sulfite species [28,29]. Upon increasing the monometallic Pd sample temperature to 300 °C, the band at 1081 cm^{-1} disappeared while the peaks at 1307 cm^{-1} and 1266 cm^{-1} shifted to 1348 cm^{-1} and 1275 cm^{-1}. The peaks at 1348 cm^{-1} and 1275 cm^{-1} were assigned to bulk aluminum sulfates [30,31]. The new peak, which evolved at 1390 cm^{-1}, was assigned to aluminum surface sulfate species [28,32,33]. To provide an example of the OMNIC software peak deconvolutions, deconvolution of this peak is included in Supplementary Information Fig. S1. The disappearance of aluminum surface sulfites coupled with aluminum sulfate formation demonstrates that the Pd sample was capable of oxidizing some molecular SO_2 and aluminum surface sulfite species to form aluminum sulfates, but no palladium sulfates [$PdSO_4$] were observed, during the temperature ramp up to 300 °C.

After SO_2 saturation at 100 °C, the spectra obtained from the 0.3 Pd-0.7 Pt sample (Fig. 5b) contained peaks at 1304 cm^{-1}, 1272 cm^{-1}, 1238 cm^{-1}, 1145 cm^{-1}, and a broad band from 1080 to 1030 cm^{-1}. This broad band was assigned to aluminum surface sulfite species [28,29]. The peak at 1238 cm^{-1} corresponds to $PdSO_4$ [30]. The peaks at 1304 cm^{-1} and 1145 cm^{-1} as well as 1272 cm^{-1} were assigned to physisorbed [26,27] and chemisorbed molecular SO_2 [26] respectively. Upon increasing the 0.3 Pd-0.7 Pt sample temperature to 300 °C, the bands at 1304 cm^{-1} and 1145 cm^{-1} disappeared due to physisorbed molecular SO_2 desorption. The peak at 1272 cm^{-1} shifted to 1280 cm^{-1}, which was assigned to bulk aluminum sulfate [31]. The peak associated with $PdSO_4$ disappeared while a new peak evolved at 1210 cm^{-1}. Since the peak at 1210 cm^{-1} corresponds to aluminum surface sulfate species [28,32,33], we deduced that the sulfates on Pd, $PdSO_4$, spilled over to the alumina support during the temperature ramp. Another new peak corresponding to aluminum surface sulfates grew in at 1381 cm^{-1} while the broad band from 1080 cm^{-1} to 1030 cm^{-1} stayed intact. These data confirm that the 0.3 Pd-0.7 Pt sample was not capable of completely oxidizing or decomposing aluminum surface sulfite species during the temperature ramp up to 300 °C but did decompose $PdSO_4$ during the temperature ramp. Note, no $PdSO_4$ was observed when characterizing the monometallic Pd sample, suggesting that Pt influences its formation.

During Pt's exposure to SO_2, physisorbed, 1304 cm^{-1}, and chemisorbed, 1268 cm^{-1}, molecular SO_2 [26] formed. After increasing the sample temperature to 300 °C, aluminum surface sulfite species formed, resulting in a wide band from ~1100 cm^{-1} to ~950 cm^{-1} [26]. The peak at 1268 cm^{-1} shifted to 1270 cm^{-1}, while new peaks at 1351 cm^{-1} and 1171 cm^{-1} appeared. The peaks at 1351 cm^{-1} and 1171 cm^{-1} were assigned to aluminum surface and bulk sulfates respectively [30]. The DRIFTS data show that Pt does not begin to oxidize sulfur species until the temperature was increased from 100 °C to 300 °C, and chemisorbed molecular SO_2 species, 1270 cm^{-1}, were still stable on Pt at 300 °C.

3.4. Sulfur regeneration methods

There were significant differences in the extent of sulfur inhibition on the CH_4 oxidation reaction as well as the sulfur release characteristics during the reactor TPO and DRIFTS TPD between
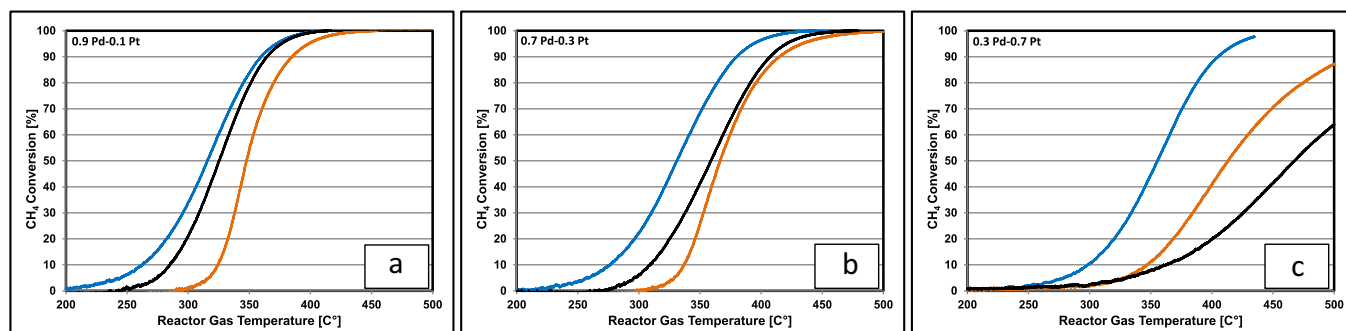
Fig. 7. Assessment of sulfur TPD regeneration effectiveness for (a) 0.9 Pd-0.1 Pt/Al$_2$O$_3$, (b) 0.7 Pd-0.3 Pt/Al$_2$O$_3$, and (c) 0.3 Pd-0.7 Pt/Al$_2$O$_3$, flowing 2000 ppm CH$_4$ and 10 vol.% O$_2$ in N$_2$, with a ramp rate of 5 °C/min after TPD to 900 °C in flowing N$_2$. Color legend defined as blue (fresh catalyst), orange (SO$_2$-treated catalyst), and black (catalyst after TPD regeneration). (For interpretation of the references to color in this figure legend, the reader is referred to the web version of this article.)

the samples. In order to evaluate how the atmosphere (inert, oxidizing, reducing) might induce sulfur species decomposition and therefore CH$_4$ oxidation recovery, TPD, TPO and TPR methods were compared.
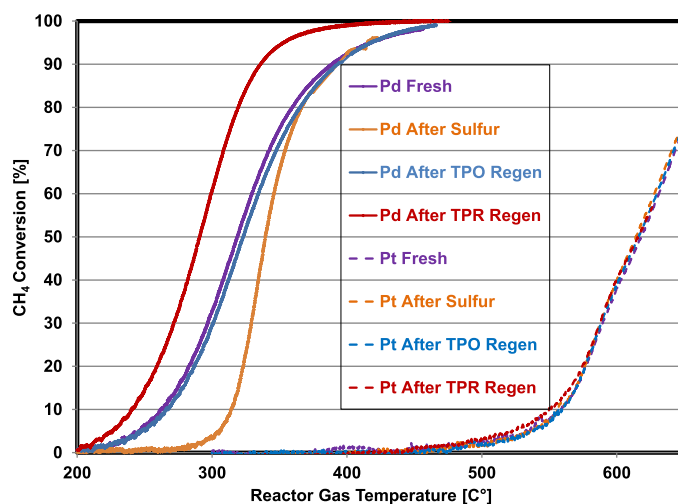
3.4.1. TPO regeneration

Since SO$_2$ was released during the CH$_4$ TPO from SO$_2$-exposed samples (Fig. 3), we suspected that some activity was recovered due to this sulfur removal. To assess the effectiveness of the TPO in removing sulfur species and recovering activity, a subsequent reference TPO was performed. To assess bimetallic decay over time on stream, a representative bimetallic catalyst sample was held under CH$_4$ oxidation reaction conditions for three 24 h intervals, each followed by two reference TPOs to assess degradation with each 24 h period. As shown in Supplementary Information Fig. 2, little decay was observed after each hold period. Based on this assessment, the TPO regeneration method (~2 h on stream) was not expected to induce any additional activity loss for the catalyst samples.

No samples, besides the Pt whose activity was unaffected by sulfur exposure, recovered their original activity after TPO regeneration. After the sulfur was released, Pd recovered the most activity (Table 2) but originally lost the most activity in comparison to the other samples. The 0.9 Pd-0.1 Pt sample lost the least activity overall and recovered slightly less activity than Pd after TPO regeneration. The 0.3 Pd-0.7 Pt sample lost the most activity overall and recovered the least activity when compared to the Pd and 0.9 Pd-0.1 Pt samples. These results show that TPO regeneration was most effective for monometallic Pd. With Pt substitution, the TPO regeneration method became less effective in recovering lost activity.

As shown in Fig. 4a, only aluminum sulfates were present on the monometallic Pd catalyst after increasing the sample temperature to 300 °C, whereas the 0.3 Pd-0.7 Pt and Pt sample still contained some aluminum surface sulfite species (Figs. 5a and 6a). It is likely that these species influenced the active sites and thus affected CH$_4$ oxidation even above 300 °C. For the 0.3 Pd-0.7 Pt sample, this competition resulted in sulfur inhibiting the CH$_4$ oxidation reaction over a larger temperature span. In the case of Pt, the CH$_4$ oxidation reaction does not begin until approximately 450 °C, and likely the sulfite species have already been oxidized or decomposed by 450 °C such that there are no other reactions or species competing with CH$_4$ oxidation in this case. We speculate that the sulfites must be associated with the precious metal sites, and since alumina-based, are located at the precious metal/support interface [34]. With their oxidation to sulfates, and the ability of the sulfate to "spillover" or migrate along or into alumina, the activity can then be regained [35].

Some SO$_2$ was released during the TPO, and some activity was recovered per subsequent TPO data review. This may have been

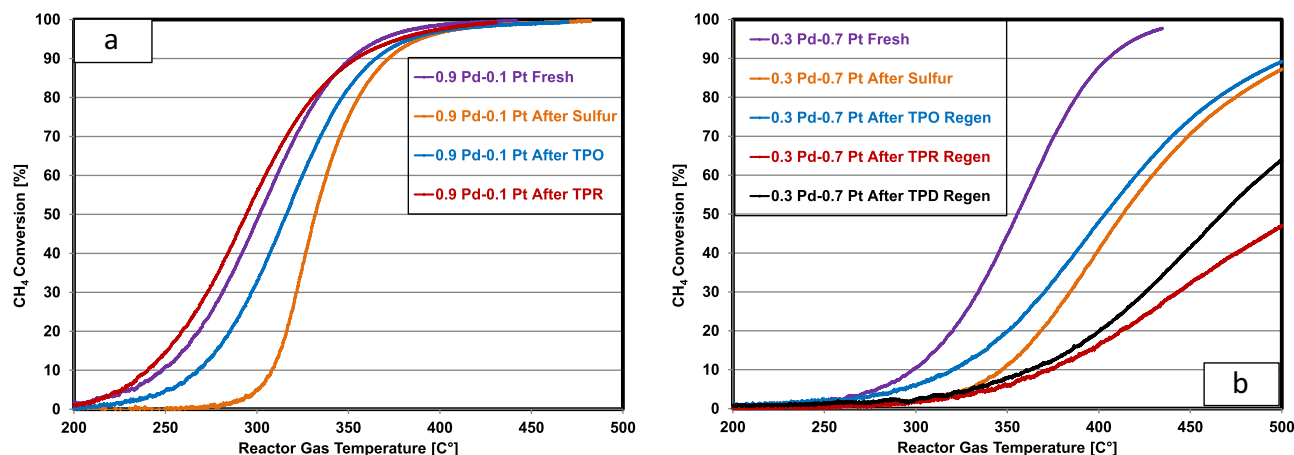associated with the chemisorbed and physisorbed SO$_2$ desorbing and some sulfite decomposition or oxidation. However, sulfate species are stable up to temperatures greater than that used for the reference TPO and could contribute to the loss in performance that persisted after the TPO. Therefore, other regeneration methods, TPD and TPR, were assessed to determine whether more activity could be recovered with partial or complete sulfate decomposition.

3.4.2. TPD regeneration

Since aluminum surface and bulk sulfates were still present on the catalysts after the low-temperature desorbing species were released (Figs. 4b, 5b, and 6b), a TPD was performed to see if activity could improve upon decomposing species stable up to ~900 °C [20]. Earlier experiments, not shown here for brevity, show that monometallic Pd catalysts displayed some loss in catalytic activity after exposure to ~900 °C in an inert gas environment. This result was not surprising because monometallic Pt and Pd catalysts are known to sinter. Since it is understood that bimetallics have some sinter resistance, TPDs were only performed on the three bimetallic samples to minimize the potential for sintering effects impacting these results. After TPD, the SO$_2$ exposed 0.9 Pd-0.1 Pt recovered more activity in comparison to the other bimetallic samples (Table 3). The 0.7 Pd-0.3 Pt sample recovered some activity after TPD, as shown in Fig. 7, whereas the 0.3 Pd-0.7 Pt sample lost even more activity. In an effort to understand why the TPD had a worse effect on the 0.3 Pd-0.7 Pt sample than the SO$_2$ exposure, a separate TPD experiment was performed with fresh bimetallic

Fig. 8. Comparison of fresh, SO$_2$-treated, and SO$_2$ regenerated monometallic catalysts, flowing 2000 ppm CH$_4$ and 10 vol.% O$_2$ in N$_2$, with a ramp rate of 5 °C/min.

Fig. 9. Comparison of fresh, SO_2-treated, and SO_2 regenerated catalysts, flowing 2000 ppm CH_4 and 10 vol.% O_2 in N_2, with a ramp rate of 5 °C/min. (a) 0.9 Pd-0.1 Pt/Al_2O_3 (b) 0.3 Pd-0.7 Pt/Al_2O_3.

samples, i.e. samples not exposed to SO_2. Proceeding in this manner was necessary in order to decouple any SO_2-exposure related decay from that related to TPD conditions.

After 900 °C exposure, each sample underwent a reference TPO and CO chemisorption experiment. The 0.9 Pd-0.1 Pt sample slightly decayed due to the 900 °C exposure (Table 4). For the 0.3 Pd-0.7 Pt sample, the activity was greatly reduced after the 900 °C exposure, to a similar extent as that observed after the TPD after SO_2 exposure. In assessing the 900 °C exposure effects on particle size (Table 4), the 0.9 Pd-0.1 Pt and 0.7 Pd-0.3 Pt sample particle sizes approximately doubled whereas the 0.3 Pd-0.7 Pt sample more than quadrupled. Although all samples sintered due to the 900 °C exposure, the TPD regeneration helped improve activity of 0.9 Pd-0.1 Pt relative to the SO_2-exposed sample performance. As more Pt was substituted for Pd, less benefit from the TPD regeneration was observed. We concluded that as more Pt was substituted into the Pd catalyst, the more the sintering effects impacted the activity in comparison to the sulfur exposure.

3.4.3. TPR regeneration

The CH_4 oxidation reaction was most inhibited over the SO_2-exposed 0.3 Pd-0.7 Pt sample, which lost even more activity after TPD regeneration due to the significant amount of sintering at 900 °C. Since research has shown that some aluminum sulfates can be reduced in H_2 at 600 °C [19], we evaluated TPR to 600 °C as a regeneration method, with sintering impacts hopefully minimized. The CH_4 oxidation activity for the SO_2-exposed Pt was unaffected by the TPR (Fig. 8). The SO_2-exposed Pd and 0.9 Pd-0.1 Pt samples not only recovered the activity lost due to sulfur exposure, but also exceeded their fresh catalyst activity (Figs. 8 and 9a). Cullis and Willatt [36] found that Pd-based catalysts achieve maximum CH_4 oxidation activity when the catalyst is first reduced then allowed to adsorb O_2 to oxidize the Pd particles to some extent prior to undergoing the CH_4 oxidation reaction. We concluded that the reduction process 1) removed sulfur species thereby recovering catalytic activity and 2) when followed by a reoxidation process, formed a more highly active oxide on the Pd and 0.9 Pd-0.1 Pt catalysts. In contrast, the SO_2-exposed 0.3 Pd-0.7 Pt activity decayed further after TPR (Fig. 9b). This decay was even greater than that observed after TPD.

Again to investigate the 0.3 Pd-0.7 Pt decay specific to the TPR temperature and independent of the SO_2-exposure, fresh samples were heated to 650 °C followed by a reference TPO to determine whether any activity loss occurred due to the high temperature

exposure. As shown in Table 4, the 0.9 Pd-0.1 Pt activity improved slightly, however, as more Pt was substituted for Pd in the bimetallic catalysts, activity was lost. Recalling the sintering observed at 900 °C (Table 4), where the PM particles in the 0.3 Pd-0.7 Pt sample grew twice as much as that of the other bimetallic particles upon 900 °C exposure, we expect that at 650 °C, some sintering also occurred and to a greater extent than the other samples. Furthermore, Müller et al. found that smaller Pd particles are more easily oxidized to form PdO in comparison to larger Pd particles [37], so sintering Pd particles coupled with a reduction process could make reoxidizing the large Pd particles more challenging.

3.4.4. Interpretation of regeneration results

During SO_2 exposure at 100 °C, sulfur species covered Pd sites (Fig. 4a) resulting in less available Pd to participate in the CH_4 oxidation reaction (Fig. 2a and 2b). Since Pd is effective at oxidizing these sulfur species to form sulfates below 300 °C (Fig. 4b), CH_4 oxidation on SO_2-exposed Pd catalysts will be inhibited at low temperatures until sulfur species have been desorbed or oxidized to form sulfates that can spillover to the support, thereby freeing up the Pd. Any remaining inhibition is due to aluminum sulfates, which require high temperatures or reduction for decomposition (Fig. 8). Since the precious metal site is the active site, the sulfates that are impacting performance are likely in close proximity to the precious metal sites, maybe at the interface between them and the alumina support, or can block pores thereby limiting access to the active sites [38,39]. In contrast, the 0.3 Pd-0.7 Pt did not completely oxidize aluminum sulfite species (Fig. 5b) below 300 °C to form aluminum sulfates. And we speculate that these sulfite species are at the alumina/metal interface and thus do influence/inhibit the oxidation reaction. Although PdSO$_4$, which formed at 100 °C, decomposed below 300 °C, the sulfite decomposition or oxidation was slow enough that inhibition still existed at/above 300 °C, until all sulfites were oxidized to form sulfates or decompose on 0.3 Pd-0.7 Pt. Similarly, no sulfites or sulfates were formed at 100 °C with monometallic Pt (Fig. 6b) and complete aluminum sulfite oxidation at 300 °C was not observed (Fig. 6b). In this case, it is unlikely that the sulfite inhibited the CH_4 oxidation reaction because even fresh Pt did not begin to oxidize CH_4 until higher temperatures (Fig. 1). As more Pt was added, less sulfite decomposition or oxidation occurred by 300 °C. We postulate that this delayed sulfite decomposition or sulfate formation also results in an increased temperature at which active sites can be regenerated via sulfur desorption, sulfate migration, or sulfate spillover.

As shown in Fig. 1, initially Pt substitution for Pd (0.9 Pd-0.1 Pt) resulted in increased CH_4 oxidation activity. Additional Pt substitution for Pd resulted in incremental reductions in activity. Recalling that the 0.9 Pd-0.1 Pt sample slightly increased in activity after 650 °C exposure and experienced a slight decay with 900 °C exposure (Table 4), we confirmed that small Pt substitution provides some sintering resistance resulting ultimately in increased activity in comparison to monometallic Pd. With further Pt substitution, 0.7 Pd-0.3 Pt, activity losses due to 650 °C and 900 °C exposure were observed. Even further substitution, 0.3 Pd-0.7 Pt, resulted in a further increase in activity loss after the 650 °C exposure, and even more so after 900 °C exposure. Since the 0.3 Pd-0.7 Pt particles grew more in comparison to the other bimetallics (Table 4), further Pt substitution beyond 0.9 Pd-0.1 Pt seemed to provide less sintering resistance. Therefore, regeneration methods requiring high temperatures are less effective for bimetallic catalysts with less than 90% Pd because benefits associated with sulfur removal could be canceled out by losses associated with sintering.

Since all catalysts were previously exposed to the reference TPO conditions, no additional sintering occurred with the TPO regeneration method, and activity was regained to various degrees for all catalysts containing Pd. SO_2-exposed Pd recovered almost all activity via TPO regeneration and increased in activity via TPR regeneration. The 0.9 Pd-0.1 Pt sample also increased in activity after TPR but did not recover all activity via TPO regeneration. As more Pt was substituted for Pd, the TPO regeneration method became less effective. This is in good agreement with the DRIFTS data (Figs. 5b and 6b) that showed catalysts with little to no Pd cannot completely decompose or oxidize sulfites to form sulfates below 300 °C. This again supports the idea that delayed sulfite decomposition or sulfate formation means an increased temperature is required for active site regeneration.

The TPD regeneration method resulted in some activity recovery for the bimetallic catalysts tested except 0.3 Pd-0.7 Pt. Similarly, the TPR regeneration method was the most effective at improving activity for 0.9 Pd-0.1 Pt but negatively impacted the 0.3 Pd-0.7 Pt activity, more than the sulfur exposure. These results again show that substituting some Pt for Pd provides some sinter and sulfur resistance in comparison to monometallic Pd. These aspects also allow SO_2-exposed bimetallics, like 0.9 Pd-0.1 Pt and 0.7 Pd-0.3 Pt, to be regenerated via TPO or TPD while only having a slightly negative impact on activity. The data collected from the 0.3 Pd-0.7 Pt sample show that substituting too much Pt for Pd results in no benefits in terms of sinter or sulfur resistance. Under the conditions tested, for Pt, CH_4 oxidation activity was not impacted by SO_2 exposure or its regeneration methods.

4. Conclusions

In this study we examined the effect of SO_2 exposure on CH_4 oxidation reaction with respect to Pd:Pt mole ratio. At 100 °C, all samples physisorbed and chemisorbed molecular SO_2 but only catalysts containing Pd also formed aluminum surface sulfite species. As increasing Pt amounts were substituted for Pd, catalysts were not capable of fully oxidizing aluminum surface sulfite species at 300 °C resulting in less sulfates formed at low temperatures. Failure to form sulfates at lower temperatures resulted in the CH_4 oxidation reaction being inhibited over a broader temperature span even after low-temperature desorbing species, i.e. molecular SO_2 and some aluminum surface sulfite species, were removed. We believe this extended inhibition was due to sulfites being on or nearby active sites thereby influencing the CH_4 oxidation reaction. In contrast, catalysts with little to no Pt substitution were able to completely decompose or oxidize sulfites at 300 °C resulting in an abundance of surface and bulk aluminum sulfates. These sul-

fates have less impact, at the levels formed in this study, possibly due to their migration away from the active sites. In this case, the CH_4 oxidation reaction was inhibited over a narrower temperature span after low-temperature desorbing species were removed or oxidized.

These differences resulted in different relative extents of sulfur inhibition and sulfur regeneration method effectiveness. The catalysts with little to no Pt substitution recovered some activity via TPO regeneration but recovered the most via TPR regeneration due to sulfate removal and optimized activity associated with the reduction-reoxidation process. Although some Pt substitution for Pd provided some sinter and sulfur resistance, substituting too much Pt for Pd resulted in neither. As a result, the $Pd_{0.3}Pt_{0.7}/Al_2O_3$ catalyst experienced the greatest decay in activity due to SO_2 exposure and declined further after high-temperature sulfur regeneration methods such as TPD and TPR. Overall, when SO_2-exposed bimetallic catalysts contain a greater amount of Pt than Pd, TPD and TPR regeneration are not effective. For these bimetallic catalysts, the presence of sulfur was less detrimental to CH_4 oxidation activity than the sintering effects associated with TPD and TPR processes.

Appendix A. Supplementary data

Supplementary data associated with this article can be found, in the online version, at http://dx.doi.org/10.1016/j.apcatb.2017.01.050.

References

[1] R.E. Hayes, R. Abbasi, L. Wu, S.E. Wanke, Chem. Eng. Res. Des. 90 (2012) 1930–1942.
[2] K.S. Varde, T. Bohr, Soc. Automot. Eng. Inc. 931632 (1993).
[3] D.L. Trimm, J.H. Lee, Fuel Process. Technol. 42 (1995).
[4] P. Gélin, M. Primet, Appl. Catal. B: Environ. 39 (2002).
[5] O. Demoulin, B.L. Clef, M. Navez, P. Ruiz, Appl. Catal. A: Gen. 344 (2008).
[6] G. Lapisardi, P. Gélin, A. Kaddouri, E. Garbowski, S. Da Costa, Top. Catal. 42–43 (2007).
[7] R. Burch, P. Loader, Appl. Catal. B: Environ. 5 (1994) 149–164.
[8] H. Yamamoto, H. Uchida, Catal. Today 45 (1998).
[9] N.M. Kinnunen, J.T. Hirvi, M. Suvanto, T.A. Pakkanen, J. Mol. Catal. A: Chem. 356 (2012).
[10] M. Skoglundh, L.O. Löwendahl, J.E. Ottersted, Appl. Catal. 77 (1991).
[11] G. Lapisardi, L. Urfels, P. Gélin, M. Primet, A. Kaddouri, E. Garbowski, S. Toppi, E. Tena, Catal. Today 117 (2006).
[12] H. Ohtsuka, Catal. Lett. 141 (2011) 413–419.
[13] P. Castellazzi, G. Groppi, P. Forzatti, Appl. Catal. B: Environ. 95 (2010) 303–311.
[14] K. Persson, A. Ersson, K. Jansson, J.L.G. Fierro, S.G. Järås, J. Catal. 243 (2006) 14–24.
[15] G. Corro, C. Cano, J.L.G. Fierro, J. Mol. Catal. A: Chem. 315 (2010) 35–42.
[16] J.K. Lampert, M.S. Kazi, R.J. Farrauto, Appl. Catal. B: Environ. 14 (1997).
[17] N. Ottinger, R. Veele, Y. Xi, Z. Liu, SAE Int. J. Engines 8 (2015) (2015-01-0991).
[18] F. Arosio, S. Colussi, G. Groppi, A. Trovarelli, Catal. Today 117 (2006) 569–576.
[19] M. Waqif, 0 Saur, J. Lavalle, S. Perathoner, C. Centi, J. Phys. Chem. 95 (1991) 4051–4058.
[20] O. Saur, M. Bensitiel, A. Mohammed Saad, J. Lavalley, C. Tripp, B. Morrow, J. Catal. 9 (1986) 104–110.
[21] T. Rades, V. Yu Borovkov, V.B. Kazansky, M. Polisset-Thfoin, J. Fraissard, J. Phys. Chem. 100 (1996) 16238–16241.
[22] Y. Zhang, Y. Cai, Y. Guo, H. Wang, L. Wang, Y. Lou, Y. Guo, G. Lu, Y. Wang, Catal. Sci. Technol. 4 (2014) 3973–3980.
[23] J. Bensalem, D. Muller, Tessier F. Bozon-Verduraz, J. Chem. SOC. Faraday Trans. Vol. 92 (17) (1996) 3233–3237.
[24] A.B. Martinez-Arias, M. Hungría, A. Fernández-García, A. Iglesias-Juez, J.A. Anderson, J.C. Conesa, J. Catal. 221 (2004) 85–92.
[25] N. Toshima, Y. Shiraishi, A. Shiotsuki, D. Ikenaga, Y. Wang, Eur. Phys. J. D 16 (2001) 209–212.
[26] A. Datta, R. Cavell, R. Tower, Z. George, J. Phys. Chem. 89 (1985) 443–449.
[27] M. Mitchell, V. Sheinker, M. White, J. Phys. Chem. 100 (1996) 7550–7557.
[28] C. Chang, J. Catal. 53 (1978) 374–385.
[29] T. Yu, H. Shaw, Appl. Catal. B: Environ. 18 (1998) 105–114.
[30] D. Mowery, R. McCormick, Appl. Catal. B: Environ. 34 (2001) 287–297.
[31] D. Bounechada, S. Fouladvand, L. Kylhammar, T. Pingel, E. Olsson, M. Skoglundh, J. Gustafson, M. Di Michiel, M. Newton, P. Carlsson, Phys. Chem. Chem. Phys. 15 (2013) 8648–8661.
[32] A. Piéplu, O. Saur, J. Lavalley, O. Legendre, C. Nedez, Catal. Rev.: Sci. Eng. 40 (4) (1998) 409–450.
[33] S. Nam, G. Gavalas, Appl. Catal. 55 (1989) 193–213.

[34] R. Burch, E. Halpin, M. Hayes, K. Ruth, J.A. Sullivan, Appl. Catal. B: Environ. 19 (1998) 199–207.
[35] J. Li, A. Kumar, X. Chen, N. Currier, A. Yezerets, SAE International Technical Paper (2013) (2013-01-0514).
[36] C.F. Cullis, B.M. Willatt, J. Catal. 83 (1983) 267–285.
[37] C. Müller, M. Maciejewski, R.A. Koeppel, A. Baike, J. Catal. 166 (1997) 36–43.
[38] A.F. Lee, K. Wilson, R.M. Lambert, C.P. Hubbard, R.G. Hurley, R.W. McCabe, H.S. Gandhi, J. Catal. 184 (1999) 491–498.
[39] J.M. Jones, V.A. Dupont, R. Brydsonb, D.J. Fullertona, N.S. Nasric, A.B. Rossa, A.V.K. Westwood, Catal. Today 81 (2003) 589–601.